JOURNAL OF PETROLOGY | VOLUME 44 | NUMBER 4 | PAGES 773–788 | 2003

Kinetics of the Coesite–Quartz Transition: Application to the Exhumation of Ultrahigh-Pressure Rocks

J. P. PERRILLAT*, I. DANIEL, J. M. LARDEAUX AND H. CARDON

LABORATOIRE DE SCIENCES DE LA TERRE, UMR 5570 CNRS–UCB LYON 1–ENS LYON, BAT. 402 GÉODE, 43 BD DU 11 NOVEMBRE 1918, 69622 VILLEURBANNE CEDEX, FRANCE

RECEIVED MARCH 22, 2002; ACCEPTED OCTOBER 29, 2002

The kinetics of the quartz–coesite phase transition has been studied in situ *by X-ray diffraction in the 2·1–3·2 GPa, 500–1010°C pressure–temperature range. Analysis of the data within Cahn's model of nucleation and growth at grain boundaries reveals that the prograde and retrograde reactions have different kinetics. The quartz → coesite transformation is one order of magnitude faster than coesite → quartz. Both reactions are characterized by high nucleation rates, so that the overall reaction kinetics is controlled by crystal growth processes. For the coesite → quartz transformation, growth rates are extrapolated using Turnbull's equation with an activation energy for the transition of 163 ± 23 kJ/mol. This kinetic law is combined with an 'inclusion in a host' elastic model to study the contribution of kinetics in coesite preservation. This numerical modelling shows that above 400°C retrograde transformation of coesite to quartz is mainly controlled by the 'pressure vessel' effect of the host phase, whereas reaction kinetics is the controlling factor at lower temperatures. The influence of the shape of the* P–T *path and the exhumation rate upon the retrogression of coesite to quartz are investigated to use the percentage of unretrogressed coesite inclusions to constrain* P–T–t *paths.*

KEY WORDS: *coesite; quartz; kinetics; ultrahigh-pressure metamorphism;* P–T–t *paths*

INTRODUCTION

The discovery of coesite (Chopin, 1984; Smith, 1984) and micro-diamonds (Sobolev & Shatsky, 1990; Dobrzhinetskaya *et al.*, 1995) in metamorphic rocks led to the definition of the ultrahigh-pressure (UHP) metamorphic facies. This facies has been now recognized world-wide in Phanerozoic orogenic domains (e.g. Coleman & Wang, 1995; Carswell, 2000), such that the burial of crustal rocks to mantle depths (>90 km) and their subsequent exhumation to the Earth's surface appears as a common process. The processes by which UHP metamorphic rocks are exhumed is still incompletely understood and several competing models exist (e.g. Ahnert, 1970; Cowan & Silling, 1978; Cloos, 1982; Platt, 1986, 1993; Andersen & Jamveit, 1990; England & Molnar, 1990; Chemenda *et al.*, 1995; Guillot *et al.*, 2000). Discriminating between these models requires comparison of pressure–temperature–time (P–T–t) paths calculated for the UHP units with those predicted by theoretical models (e.g. Duchêne *et al.*, 1997). In particular, these P–T–t paths should allow the survival of high-pressure minerals such as coesite. The partial preservation of coesite is commonly explained by its inclusion in a host phase that acts as a 'pressure vessel'. Purely elastic models based on the internal pressure in the inclusion (Gillet *et al.*, 1984; Van der Molen & Van Roermund, 1986) allow degrees of retrogression, in agreement with those observed in natural samples, to be calculated. However, these models do not take into account the kinetics of the coesite–quartz transformation, which might be a controlling factor. Kinetic data for this transition are scarce; only four recent studies (Zinn *et al.*, 1995, 1997*a*, 1997*b*; Mosenfelder & Bohlen, 1997) and an earlier one by Babich *et al.* (1989) are reported in the literature and display different kinetics.

*Corresponding author. Telephone: +33 (0)4 72 44 84 90. Fax: +33 (0)4 72 44 85 93. E-mail: Jean-Philippe.Perrillat@univ-lyon1.fr

The purpose of this contribution is first to present new kinetic data on the coesite–quartz transformation obtained by *in situ* X-ray diffraction using synchrotron radiation (Skelton *et al*., 1983; Will & Lauterjung, 1987). We analyse the kinetic data using the model of grain boundary nucleation and interface-controlled growth of Cahn (1956), which allows us to determine the kinetic law of the coesite to quartz transformation. This kinetic law is then combined with an 'inclusion in a host' elastic model to calculate the percentage of transformation of a coesite inclusion in a pyrope-rich garnet from the French Massif Central (Monts du Lyonnais UHP unit). The influence of the shape of the P–T paths and the exhumation rate upon the degree of retrogression of coesite to quartz is investigated to use the percentage of unretrogressed coesite as a new constraint for the construction of P–T–t paths.

EXPERIMENTAL AND ANALYTICAL METHODS

Starting material

To study the influence of grain size on kinetics, two types of samples were used. The first type was a micronic powder of α-quartz (grain diameter of 1–2 μm) intimately mixed with 5 wt % of NaCl + Au powder. This material has a OH content lower than 100×10^{-6} H/Si. This powder was pressed and heated simultaneously in the 500–1100°C, 2–3 GPa range, within the stability field of α-quartz. During this annealing time, grain growth eliminated small grains, elastic strain was relaxed and high dislocation densities were reduced to obtain relaxed grains 2–10 μm in diameter (samples 1–3). The second type consisted of two cylinders of Suprasil® (synthetic dry type) silica glass (l = 1·45 mm, ∅ = 1·5 mm) separated by a 50 μm layer of NaCl + Au powder. This glass has a low OH content of 10×10^{-6} H/Si. It was subjected to P–T conditions in the coesite stability field for grain growth, until the coesite diffraction lines were observed. This procedure led to a grain size of 50 μm (samples 4 and 5).

Experimental apparatus

Experiments were performed at the DW11 beamline of the Laboratoire pour l'Utilisation du Rayonnement Electromagnétique (LURE, Orsay, France) by energy dispersive X-ray (EDX) diffraction. The energy profile of the incident beam allowed diffraction patterns to be collected over the energy range 10–60 keV. The polychromatic beam was collimated to dimensions of 100 μm × 50 μm. Diffracted X-rays were recorded by a solid-state multichannel Ge detector at a fixed angle of $2\theta = 6{\cdot}3°$.

The use of a Paris–Edinburgh vessel (Besson *et al*., 1992) allows the application of hydrostatic pressures up to 7 GPa and temperatures up to 2000°C on an experimental volume of several cubic millimetres. As a consequence of this large experimental volume, combined with the high brilliance of the synchrotron radiation, diffraction patterns could be collected within 30–60 s. The cell assembly, placed between two anvils, was made of three main parts: the pressure-transmitting medium, the heating device, and the sample. The pressure transmitting medium consisted of a mixture of amorphous boron and epoxy resin. As its deformation is almost reversible (Le Godec, 1999), it is possible to work also along decompression paths. Consequently, measurements on several pressure cycles were made. The heating device was a cylindrical graphite furnace connected to a high-intensity power supply. Temperature was adjusted rapidly by varying the electrical power delivered to the furnace. The internal volume of the furnace was about 6 mm^3 (l = 3 mm, ∅ = 1·5 mm).

Temperature was measured by a K-type thermocouple in contact with the sample. The temperature gradient in the cell assembly was estimated by numerical modelling to be of the order of 10°C/mm at 700°C (Hammi, 1995). The temperature uncertainty was estimated to be ±20°C. To determine the pressure *in situ*, a powder of NaCl + Au was added to the sample as an internal pressure standard. Pressure was calculated from Vinet's equation of state (Vinet *et al*., 1987) for NaCl and Au using the estimated temperature and lattice parameters determined from X-ray diffraction patterns acquired periodically during each experiment. Unit-cell parameters and the volume of NaCl and Au were refined by a least-squares fitting technique using respectively the (111), (200), (220), (222) and the (111), (200), (220), (311) diffraction lines. The estimates using either NaCl or Au give nearly similar results (the difference between the two estimates being generally lower than the pressure uncertainty). The pressure uncertainty, related to discrepancies in the positioning of standard diffraction lines and propagation of temperature uncertainty, is considered to be ±0·1 GPa.

Experimental procedure

After synthesis, the samples were subjected to the P–T conditions required for the kinetic experiment. The high-pressure cell was carefully aligned with respect to the X-ray set-up and kept at constant position. The P–T path followed during an experiment is schematically shown in Fig. 1. In the case of the quartz → coesite transformation, once the sample was under high pressure and temperature, close to the coesite–quartz

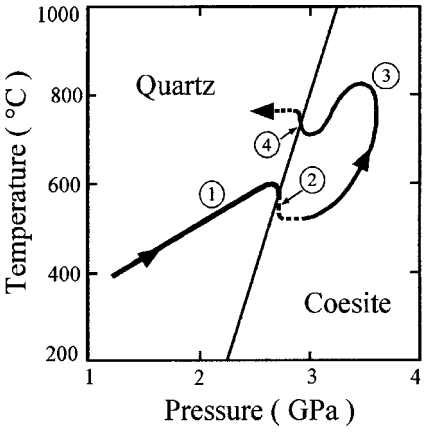

Fig. 1. Representative experimental P–T path. Numbers refer to (1) pressure and temperature rise, (2) isobaric cooling, (3) high-temperature stage, (4) isobaric heating. The same sample was cycled several times across the quartz–coesite transition.

equilibrium, the temperature was allowed to fall slightly until the first coesite diffraction lines were observed. The P–T conditions were then held constant as long as the transition proceeded. After complete phase transformation (i.e. when quartz diffraction lines disappear), pressure was increased and temperature raised to achieve the completion of the reaction throughout the sample volume. A similar procedure was used to study the coesite → quartz transition. As a consequence of the purely elastic behaviour of the pressure-transmitting medium, several prograde and retrograde transformations could be studied within the same sample. During transition, X-ray diffraction patterns were collected every 1–3 min with a counting time for each pattern of 30–60 s. Even for the shortest counting times, the diffraction patterns showed a good resolution and a high signal-to-noise ratio. At the end of each experiment, the temperature was allowed to fall quickly (25°C/min) to quench the sample texture. Pressure was decreased progressively (50 MPa/min) to prevent crack formation in the sample. The recovered samples were then prepared for SEM study to estimate grain size.

Data processing

Seven coesite → quartz and five quartz → coesite transitions were achieved in the pressure range 2·1–3·2 GPa and the temperature range 500–1010°C (Table 1). The degree of transformation X can be estimated from the relative intensity of the quartz and coesite diffraction peaks. For each peak, the position (i.e. the energy in keV) and the intensity at peak maximum (i.e. peak height, in number of photons/m^2/s) were evaluated by fitting the diffraction spectra with Gaussian curves, after background subtraction. As the conditions of spectrum acquisition (i.e. counting time, intensity of incident X-rays) varied with time, intensities were normalized to the intensity of the $\beta_4 L_I M_{II}$ fluorescence X-ray of Au. The degree of transformation $X(t)$ is thus calculated as

$$1 - X(t) = \frac{I_{at}}{I_{a0}} \qquad (1)$$

where I_{at} is the normalized intensity of the highest diffraction peak for phase a [(040) coesite or (101) quartz] at time t, and I_{a0} is the value at time $t = 0$. When possible, the degree of transformation is also calculated using the (112) (100) quartz or the (031) (021) coesite diffraction lines. For experiments below 900°C, both methods give similar results, demonstrating the lack of preferred orientation; preferred orientations do, however, seem to develop in experiments above 900°C.

Figure 2a and b illustrates the transformation–time data obtained in the experiments. These data show a good time resolution, of the order of a minute, and a low uncertainty in the degree of transformation, as low as 0·05–0·1 for experiments up to 900°C. The uncertainty is mainly linked to the error propagation on the intensity of the diffraction peaks.

ANALYSIS OF THE KINETIC DATA

Relative influence of nucleation and growth

The formation of a new phase in the sample results from a combination of nucleation and growth processes whose relative influence on kinetics must be determined. The kinetics of polymorphic phase transitions is usually described using the Avrami equation (Avrami, 1939) which expresses the degree of transformation X as a function of time t:

$$X(t) = 1 - \exp(kt^n) \qquad (2)$$

where k and n are constants whose values depend on the relative importance of nucleation and growth. A modified form of this equation for isobaric–isothermal interface-controlled transformations has been proposed by Cahn (1956):

$$X(t) = 1 - \exp\left[-2S\int_0^{y'}[1 - \exp(-z)\mathrm{d}y]\right] \qquad (3)$$

where

$$z = \pi\int_0^{t-t'} N[x'^2(t - \tau)^2 - y^2]\mathrm{d}\tau$$

N is the nucleation rate at grain boundaries, x' is the growth rate of the product phase, S is the grain boundary area, $y' = x't$ is the growth distance after time t, τ is the time at which a nucleus forms, and t' is

Table 1: Experimental conditions and results

Sample	Reaction	Pressure (GPa) (±0·1)	Temperature (°C) (±20)	Pressure overstep* (GPa)		Duration (min)	Grain size (μm)	Degree of transformation (%)
				(a)	(b)			
3	Qtz → Coe	2·8	500	0·28	0·07	30	5	0
3	Qtz → Coe	3·1	550	0·53	0·32	536	5	~90
2	Qtz → Coe	3·0	700	0·38	0·20	84	5	100
2	Qtz → Coe	2·8	800	0·02	−0·15	172	5	100
2	Qtz → Coe	3·2	900	0·36	0·19	119	5	~80
3	Coe → Qtz	2·2	550	0·35	0·55	180	5	0
1	Coe → Qtz	2·6	600	−0·02	0·18	606	2	100
2	Coe → Qtz	2·3	700	0·31	0·50	655	5	~90
2	Coe → Qtz	2·5	800	0·30	0·48	255	5	~100
3	Coe → Qtz	2·4	900	0·44	0·62	10	5	95
4	Coe → Qtz	2·8	910	0·06	0·23	575	50	100
5	Coe → Qtz	2·9	1010	0·04	0·20	14	50	100

The degree of transformation is estimated from the X-ray diffraction spectra. Duration is the time during which the sample was kept at the given temperature and pressure.
*Pressure overstep with respect to the coesite–quartz equilibrium of (a) Mirwald & Massonne (1980), (b) Bose & Ganguly (1995).

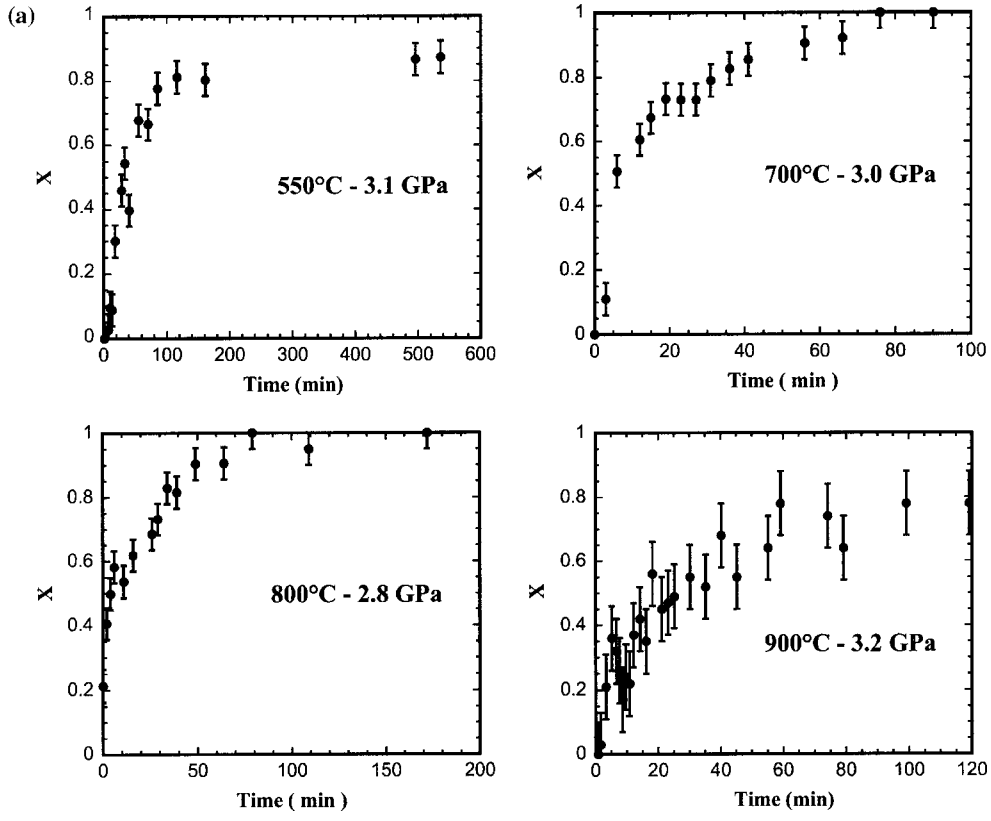

Fig. 2.

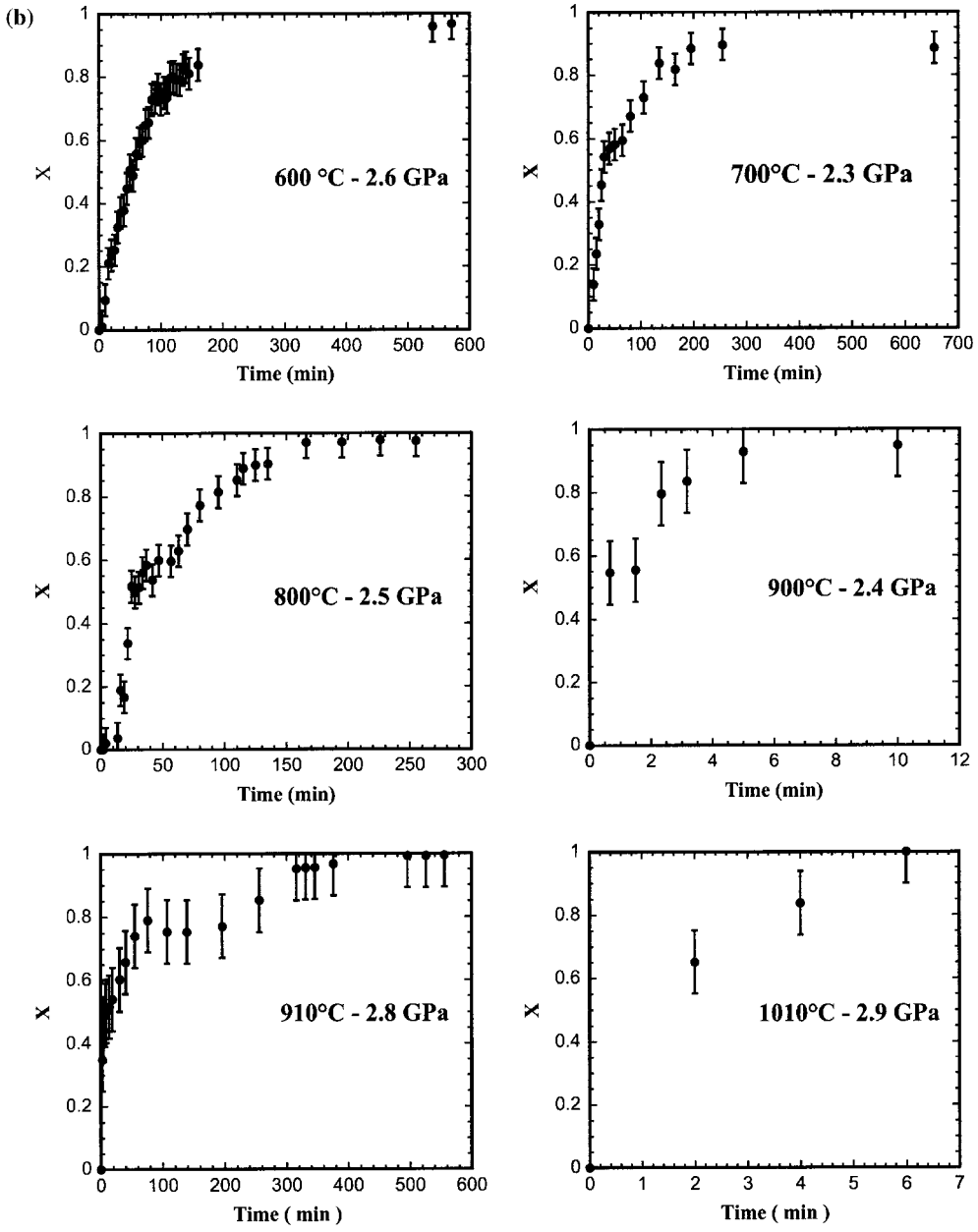

Fig. 2. Transformation–time data at specific temperatures and pressures: (a) for the quartz → coesite transition; (b) for the coesite → quartz transition.

the necessary time for a nucleus to grow to radius y. This model relies on a steady-state transformation scheme with both nucleation and growth rates constant. Two limiting cases have been discussed by Cahn (1956). Before site saturation (i.e. before the nucleation sites on the grain surface are exhausted), the kinetic equation (3) can be expressed as

$$X(t) = 1 - \exp\left[-\left(\frac{\pi}{3}\right)\mathrm{N}x'^3t^4\right]. \qquad (4)$$

After site saturation, the transformation proceeds only by growth, and equation (3) becomes

$$X(t) = 1 - \exp(-2Sx't). \qquad (5)$$

Comparing equations (4) and (5) with the Avrami equation (2), we see that the value of k varies between $[-(\pi/3)Nx'^3]$ and $[-2Sx']$ for the two limiting cases. Similarly, n varies between one and four for instantaneous and slow nucleation, respectively.

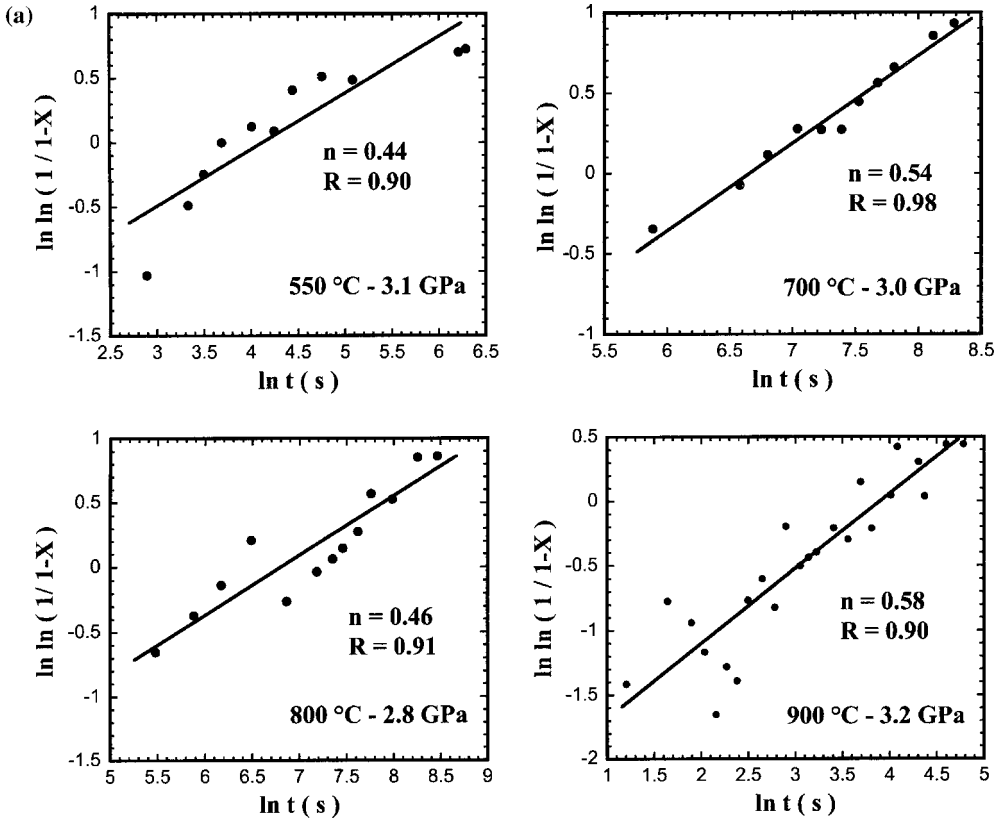

Fig. 3.

The values of n for our experimental data have been determined from the slope of plots of $\ln\{\ln[1/(1-X)]\}$ against $\ln(t)$ (Fig. 3a and b). Linear least-square fits to these data give values of n in the 0·44–0·58 range for prograde transitions, and in the 0·42–1·09 range for retrograde transitions. The n values can be alternatively deduced by adjusting the k and n parameters of the Avrami equation to the $X(t)$ data (Table 2). Both methods led to similar results, and to n values always close to or lower than one, indicating a high nucleation rate for both prograde and retrograde transformations. Values for n below the theoretically lowest value of one have already been reported by Rubie *et al.* (1990) in their study of the Ni_2SiO_4 olivine–spinel transformation and can be related to the weakness of the simple model of Cahn to describe data with accuracy. This very fast nucleation is confirmed by the strong slope of the $X(t)$ curves during the first stages of transformation (Fig. 2). The addition of a NaCl + Au powder to the sample does not seem to affect the nucleation rate, as there are no significant differences in the n values and the shape of $X(t)$ curves between experiments where the NaCl + Au powder is mixed with the α-quartz and those where it is placed as a layer between cylinders of Suprasil glass. The overall kinetics of transformation is thus controlled by growth processes. As a consequence, our study focuses on the determination of growth rates at various P–T conditions.

Determination of growth rates

Growth rates (x') at isobaric and isothermal conditions are calculated by fitting the $X(t)$ data to equation (5) with a linear regression algorithm minimizing a χ^2 function. The grain boundary surface area S is taken as $S = 3{\cdot}35/d$, where d is the mean grain size of each sample, estimated from SEM observations (Table 1). Although established for tetrakaidecahedral grains, this relation leads to reasonable values of S for most shapes (Liu & Yund, 1993). The best fits, together with the optimized value for x' and the χ^2 value, are displayed in Fig. 4a and b. Interestingly, the transformation–time data do not show a random scatter around the fitted Cahn curve, but often lie below this curve in the last stages of transformation. This indicates a decrease in growth rates that is not considered in the Cahn model based on the assumption of constant

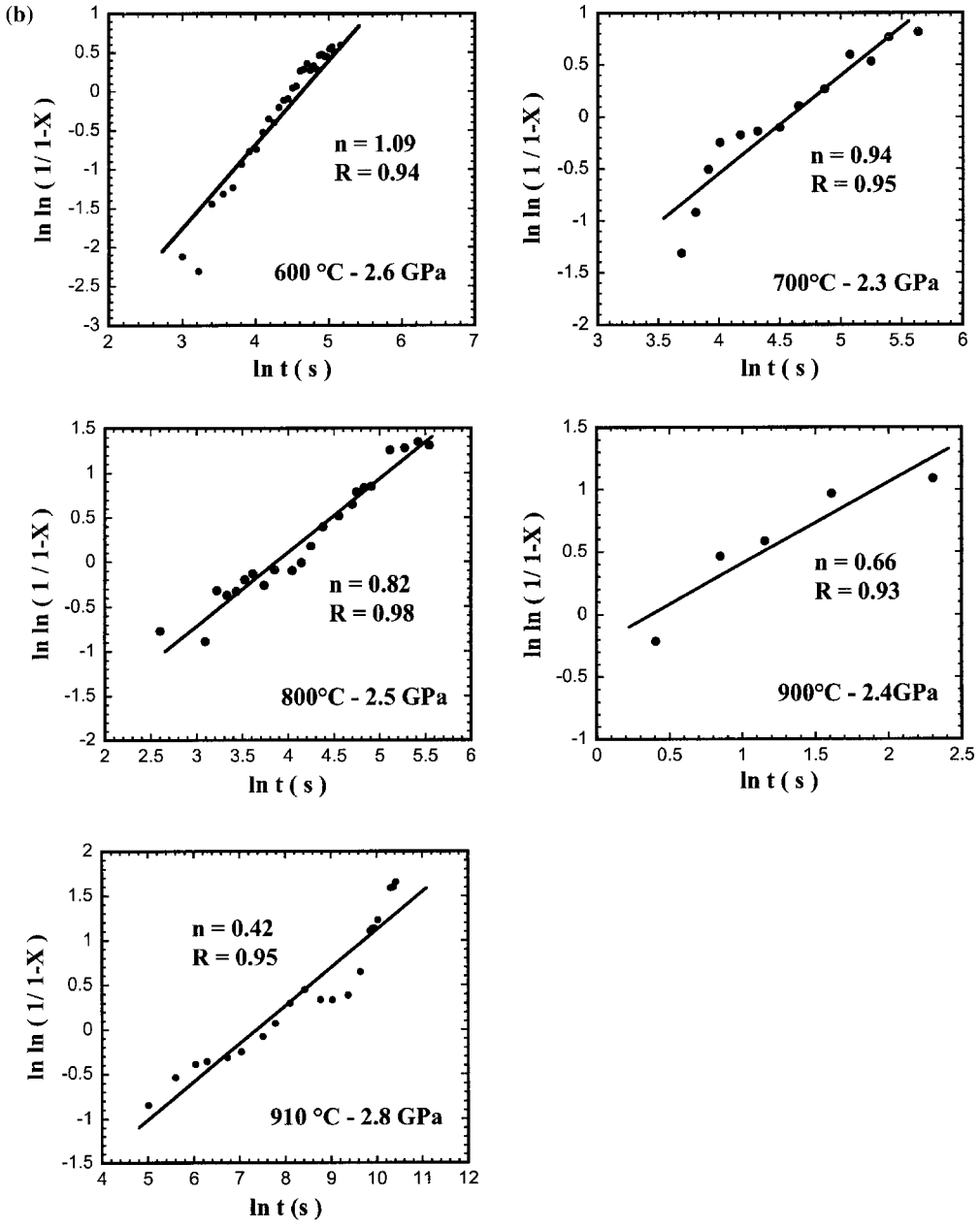

Fig. 3. Ln(t) vs ln{ln[1/(1 − X)]} plots. The slope n of the straight lines defined by the data and the correlation coefficient R are shown. (a) Quartz → coesite transition; (b) coesite → quartz transition.

growth. This decrease in growth rates may be caused by grain impingement or the development of transformation stress.

The study of growth rates results in two major conclusions. First, prograde and retrograde reactions have different kinetics. The quartz → coesite transformation is more or less one order of magnitude faster than the coesite → quartz transformation. For example, at 700°C the growth rate is $7{\cdot}9 \times 10^{-10}$ m/s for the quartz → coesite transition and $4{\cdot}1 \times 10^{-10}$ m/s for the coesite → quartz transition. Second, crystal growth appears to be a thermally activated process. Indeed, growth rates range from $4{\cdot}1 \times 10^{-11}$ m/s at 600°C to $6{\cdot}4 \times 10^{-8}$ m/s at 1010°C for the coesite → quartz transformation. Plotted in an Arrhenius diagram of $\ln(x')$ vs $1000/T$ (Fig. 5), growth rates plot along a straight line, showing an exponential dependence of growth rates on temperature.

Table 2: Comparison between n *exponents obtained by fits or graphically*

Sample	Transition	Pressure (GPa)	Temperature (°C)	*k* constant	*n* exponent	
					(a)	(b)
3	Qtz → Coe	2·8	500	—	—	—
3	Qtz → Coe	3·1	550	3·1 (±1·6) × 10^{-4}	0·96 (±0·1)	0·44
2	Qtz → Coe	3·0	700	2·3 (±0·5) × 10^{-3}	0·73 (±0·1)	0·54
2	Qtz → Coe	2·8	800	5·9 (±1·4) × 10^{-3}	0·42 (±0·1)	0·46
2	Qtz → Coe	3·2	900	1·5 (±0·3) × 10^{-3}	0·61 (±0·1)	0·58
3	Coe → Qtz	2·1	550	—	—	—
1	Coe → Qtz	2·6	600	5·2 (±2·0) × 10^{-3}	1·70 (±0·1)	1·09
2	Coe → Qtz	2·3	700	9·2 (±2·0) × 10^{-4}	0·69 (±0·1)	0·94
2	Coe → Qtz	2·5	800	3·0 (±0·9) × 10^{-4}	1·00 (±0·1)	0·82
3	Coe → Qtz	2·4	900	—	—	0·66
4	Coe → Qtz	2·8	910	36·8 (±14·0) × 10^{-3}	0·62 (±0·1)	0·42
5	Coe → Qtz	2·9	1010	—	—	—

(a) *n* exponent estimated by fitting data to the Avrami equation. The *k* constant value associated with this fit is shown. (b) *n* exponent calculated from the slope of a $\ln\{\ln[1/(1-X)]\}$ vs $\ln(t)$ diagram.

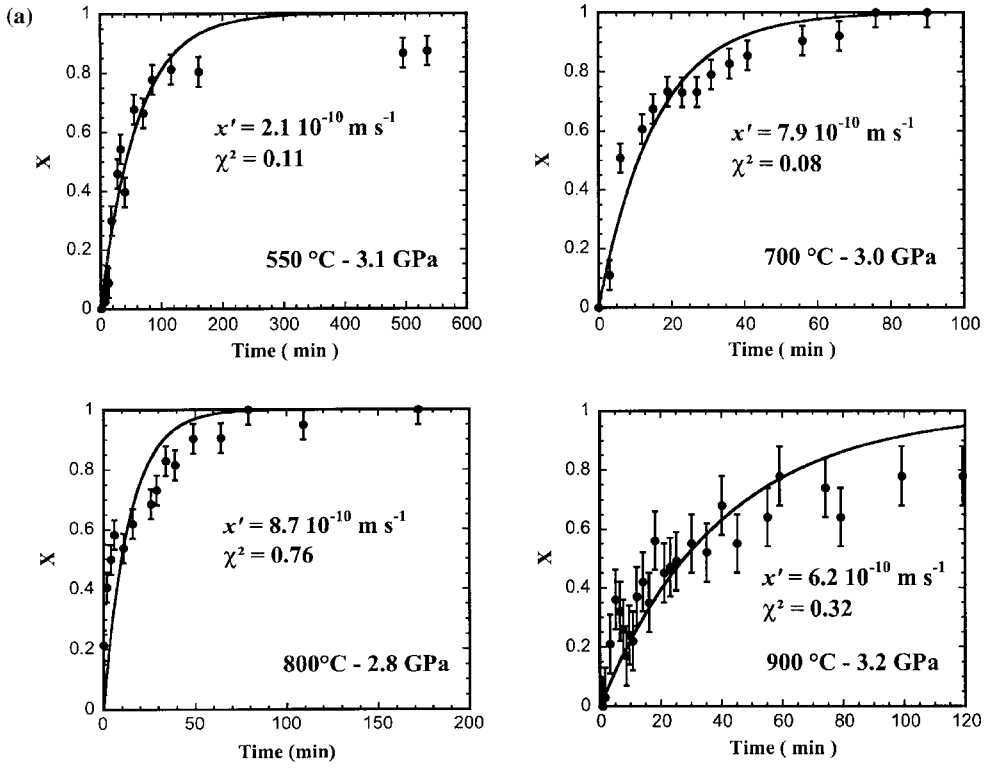

Fig. 4.

Extrapolation of growth rates

The application of the above experimental results to natural cases requires the extrapolation of measured growth rates at any P–T conditions, assuming the transformation mechanism is unchanged. This assumption is valid in the temperature range investigated in the experiments but is questionable at lower temperatures. An expression of the growth rate for the

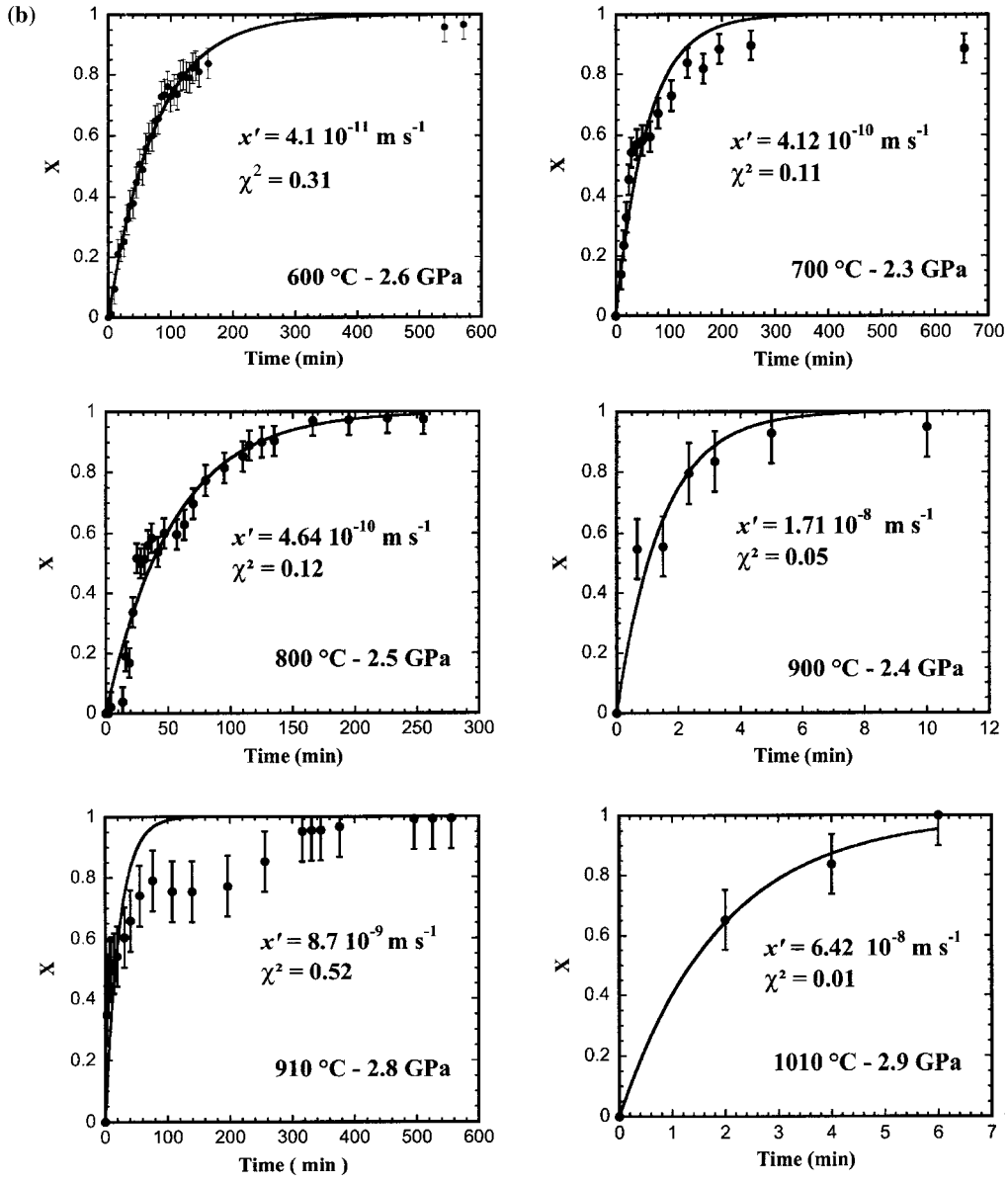

Fig. 4. Transformation–time curves obtained by fitting the experimental data to equation (5). Optimized values of growth rates (x') are shown together with the χ^2 value. (a) Quartz → coesite transition; (b) coesite → quartz transition.

product phase in an interface-controlled polymorphic phase transformation has been proposed by Turnbull (1956):

$$x' = k_0 T \exp\left(-\frac{Q}{RT}\right) \cdot \left[1 - \exp\left(-\frac{\Delta G_r}{RT}\right)\right] \quad (6)$$

where k_0 is a constant, T is the temperature, R is the gas constant, Q is the activation energy for growth and ΔG_r is the free energy change of reaction at given P–T. The ΔG_r values are calculated from the thermodynamic data of Robie *et al.* (1978) and Saxena *et al.* (1993). The k_0 and Q values are estimated from the slope and the intercept of a least-squares linear fit to the growth rate data on an $\ln\{x'/T[1 - \exp(-\Delta G_r/RT)]\}$ vs $1000/T$ plot. For the coesite → quartz transition (Fig. 5) a slope of 19·6 is calculated with a correlation coefficient $R = 0{\cdot}94$, giving a value for Q of 163 ± 23 kJ/mol. The intercept gives a value for k_0 of $2\ (\pm 1) \times 10^{-3}$. Equation (6) is then used to extrapolate the growth rate of coesite over a wide range of P–T conditions (Fig. 6). These growth rates are equivalent to speeds of reaction if nucleation can be considered instantaneous, as in our experiments. The shape of

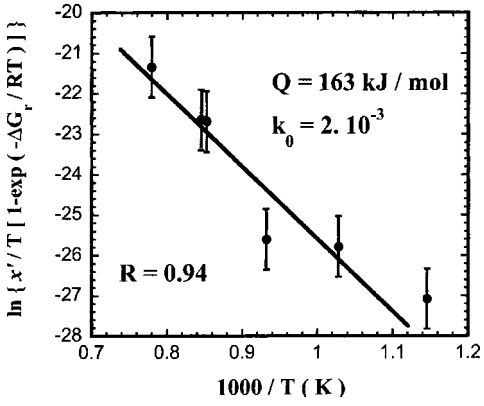

Fig. 5. Arrhenius diagram showing the exponential dependence of growth rates (x') on temperature. k_0 is the exponential of the origin ordinate, R the correlation coefficient.

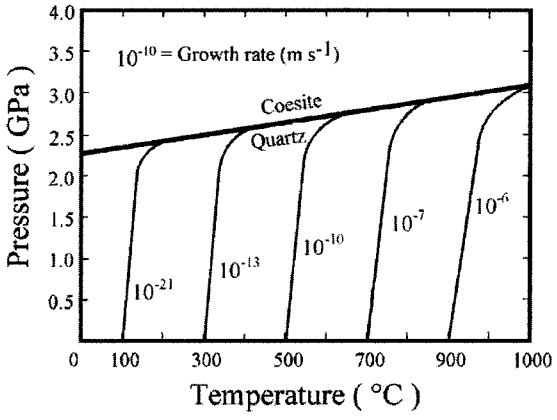

Fig. 6. Iso-growth rates curves extrapolated from the Turnbull equation (Turnbull, 1956) using the activation energy (Q) of 163 kJ/mol estimated for the coesite → quartz transition. Growth rates are expressed in m/s.

iso-growth rate curves clearly shows the exponential dependence on temperature. The pressure dependence is weaker and mainly acts close to the coesite–quartz equilibrium.

Comparison with previous studies

The kinetics of the coesite–quartz transition has already been investigated by Babich *et al.* (1989) using thermal destabilization of coesite, Zinn *et al.* (1995, 1997*a*, 1997*b*) using *in situ* X-ray diffraction, and Mosenfelder & Bohlen (1997) using the quench technique. As in our study, these previous works stressed the importance of a very fast nucleation stage and a thermally activated transformation. Babich *et al.* (1989) reported rates of transformation from coesite to quartz several orders of magnitude slower than ours, and much more dependent on pressure. For example,

Table 3: Coesite → quartz growth rates from the data of Mosenfelder & Bohlen (1997)

Temperature (°C)	Pressure (GPa)	Growth rate (m/s)	
		(a)	(b)
800	2·59	$7{\cdot}9 \times 10^{-12}$	—
800	2·38	$2{\cdot}7 \times 10^{-11}$	$1{\cdot}8 \times 10^{-11}$
850	2·63	$3{\cdot}1 \times 10^{-11}$	$2{\cdot}1 \times 10^{-11}$
900	2·67	$2{\cdot}4 \times 10^{-10}$	$1{\cdot}6 \times 10^{-10}$
1000	2·81	$6{\cdot}8 \times 10^{-10}$	$4{\cdot}5 \times 10^{-10}$

(a) Mosenfelder & Bohlen (1997) data. (b) Growth rates calculated by fitting Mosenfelder & Bohlen (1997) data using equation (5).

a rate of transformation of 1 mm/Myr was calculated for a temperature of 850°C, at 1·5 GPa. However, these results were obtained by extrapolation of thermally activated transformation of coesite at ambient pressure and hence are subject to caution. Mosenfelder & Bohlen (1997), analysing their data within Cahn's model, calculated growth rates for the coesite → quartz transition one order of magnitude slower than ours. To explain this difference, we first question data analysis. Mosenfelder & Bohlen (1997) adjusted their $X(t)$ data to equation (3) with N and x' used as fitting parameters; whereas we fit our data to equation (5) so that only the x' value is determined. We have reanalysed the original data of Mosenfelder & Bohlen (1997) using the procedure described above. Growth rates calculated (Table 3) are similar to those obtained by Mosenfelder & Bohlen, indicative of a real difference in reaction kinetics. This result emphasizes the non-influence of nucleation, as taking it into account or not yields similar results for growth rates. Second, we checked if this difference in growth rate can be linked with the different grain sizes characteristic of each experiment. No notable effect of grain size is revealed in our experiments between runs using the 2–10 μm or the 50 μm samples. Grain-size reduction results theoretically in an increase in surface energy favourable to the nucleation process (e.g. Lasaga, 1998). However, as the kinetics of the coesite–quartz transition is controlled by grain growth, grain size has little influence. In conclusion, we consider that the experimental procedure seems to be the source of the difference. In our experiments the sample was subjected to several prograde and retrograde transitions. This polyphase treatment could lead to the accumulation of defects, which might speed up the transformation (Rubie *et al.*, 1990).

The activation energy for growth (Q) was estimated by Mosenfelder & Bohlen to be 269 ± 26 kJ/mol; more than 100 kJ/mol higher than our value of 163 kJ/mol. The accumulation of defects in the sample would also reduce the activation energy.

APPLICATION OF THE KINETIC RESULTS TO NATURAL EXAMPLES

The coesite–quartz kinetic law is used to numerically model the role of kinetics in the preservation of coesite in UHP metamorphic rocks. The influence of the P–T path's shape and exhumation rate upon retrogression is also investigated.

Numerical model

Both the kinetics of the coesite → quartz transformation and the elastic model for a coesite inclusion in a host mineral are taken into account. As pointed out by Gillet *et al.* (1984) and Van der Molen & Van Roermund (1986), the host mineral acts as a 'pressure vessel' that maintains a high internal pressure on the coesite inclusion and thus prevents its retrogression. The model assumes that the host mineral remains unfractured until it reaches the surface. Consequently, the internal pressure (P_{in}) on the inclusion and the speed of the coesite–quartz transition are calculated for each P–T–t step of the exhumation path.

The internal pressure is computed using the analytical method proposed by Zhang (1998). This approach is based on the following hypotheses: (1) the host phase and the coesite inclusion are of spherical shape; (2) the inclusion is centred in the host mineral; (3) the host-inclusion temperature is homogeneous; (4) inclusion and host have a purely elastic behaviour; (5) when the inclusion-host system formed (i.e. at P_0, T_0) the internal pressure was uniform. The pressure on the inclusion (P_{in}) is given by the relation

$$P_{\mathrm{in}} = \left[\frac{1}{K_{\mathrm{i}(T,P_{\mathrm{in}})}} + \frac{x}{(1-x)K_{\mathrm{h}(T,P)}} + \frac{3}{4(1-x)\mu_{\mathrm{h}(T,P)}}\right]^{-1} \times \left\{P_0\left[\frac{1}{K_{\mathrm{i}(T,P_{\mathrm{in}})}} - \frac{1}{K_{\mathrm{h}(T,P)}}\right] + [\alpha_{\mathrm{i}(T,P_{\mathrm{in}})} - \alpha_{\mathrm{h}(T,P)}]\Delta T + \frac{P}{1-x}\left[\frac{1}{K_{\mathrm{h}(T,P)}} + \frac{3}{4\mu_{\mathrm{h}(T,P)}}\right]\right\} \quad (7)$$

where $x = R_{\mathrm{i}}^3/R_{\mathrm{h}}^3 \approx R_{\mathrm{i}0}^3/R_{\mathrm{h}0}^3$ (R_{i} and $R_{\mathrm{i}0}$ are the inclusion radius at T, P and T_0, P_0, respectively; R_{h} and $R_{\mathrm{h}0}$ are the host radius at T, P and T_0, P_0, respectively), K_{i} and K_{h} are the inclusion and host bulk modulus, α_{i} and α_{h} are their thermal expansion, and μ_{h} is the host shear modulus. Within the P–T range considered, the elastic constants can be written

$$a_{\mathrm{i}_{(T,P)}} = (a_{\mathrm{i}})_0 + \left(\frac{\partial a_{\mathrm{i}}}{\partial T}\right)T + \left(\frac{\partial a_{\mathrm{i}}}{\partial P}\right)P$$

with $a_{\mathrm{i}} = \alpha$, K, μ, and their first P and T derivatives taken as constant.

Equation (7) is solved by iteration, starting with the inclusion elastic parameters at external pressure. Elastic parameters and internal pressure are refined in this way until convergence is achieved.

In a second stage, the model calculates the free energy change (ΔG_{r}) of the coesite → quartz reaction at P_{in}, T, using the available thermodynamic data for quartz and coesite (Robie *et al.*, 1978; Saxena *et al.*, 1993). Depending on the sign of ΔG_{r}, the transition proceeds or not. If ΔG_{r} is negative a growth rate (x') is calculated using equation (6) with the Q and k_0 values determined above. The use of equation (6) relies on two hypotheses: (1) the nucleation is instantaneous on geological time scale; (2) quartz growth is confined to grain boundaries. Both hypotheses are justified by the retrogression textures of coesite inclusions (Fig. 7). Indeed, coesite inclusions are always surrounded by an inversion rim of polycrystalline quartz. This 'palisade' texture indicates the nucleation and growth of quartz at the coesite–host mineral interface and suggests a high nucleation rate.

The radial thickness of palisade quartz is then computed by multiplying the growth rate by the iteration time step. To account for the overpressure created by the volume increase at the coesite → quartz transition ($\Delta V/V = 7{\cdot}4\%$ at 50°C, 2 GPa; 13% at 800°C, 3 GPa), an additional term is inserted in equation (7):

$$P_{t\varphi} \approx x_r\left[\frac{\Delta V_{\mathrm{mol}(T,P_{\mathrm{in}})}}{V^{\mathrm{coe}}_{\mathrm{mol}(T,P_{\mathrm{in}})}}\right]$$

where x_r is the fraction of coesite retrogressed into quartz, and ΔV_{mol} the molar volume variation between the two phases. Equation (7) becomes

$$P_{\mathrm{in}} = \left[\frac{1}{K_{\mathrm{i}(T,P_{\mathrm{in}})}} + \frac{x}{(1-x)K_{\mathrm{h}(T,P)}} + \frac{3}{4(1-x)\mu_{\mathrm{h}(T,P)}}\right]^{-1} \times \left\{P_0\left[\frac{1}{K_{\mathrm{i}(T,P_{\mathrm{in}})}} - \frac{1}{K_{\mathrm{h}(T,P)}}\right] + [\alpha_{\mathrm{i}(T,P_{\mathrm{in}})} - \alpha_{\mathrm{h}(T,P)}]\Delta T + x_r\left[\frac{\Delta V_{\mathrm{mol}(T,P_{\mathrm{in}})}}{V^{\mathrm{coe}}_{\mathrm{mol}(T,P_{\mathrm{in}})}}\right] + \frac{P}{1-x}\left[\frac{1}{K_{\mathrm{h}(T,P)}} + \frac{3}{4\mu_{\mathrm{h}(T,P)}}\right]\right\}. \quad (8)$$

The evolution in size of a coesite inclusion can be followed throughout the entire exhumation path.

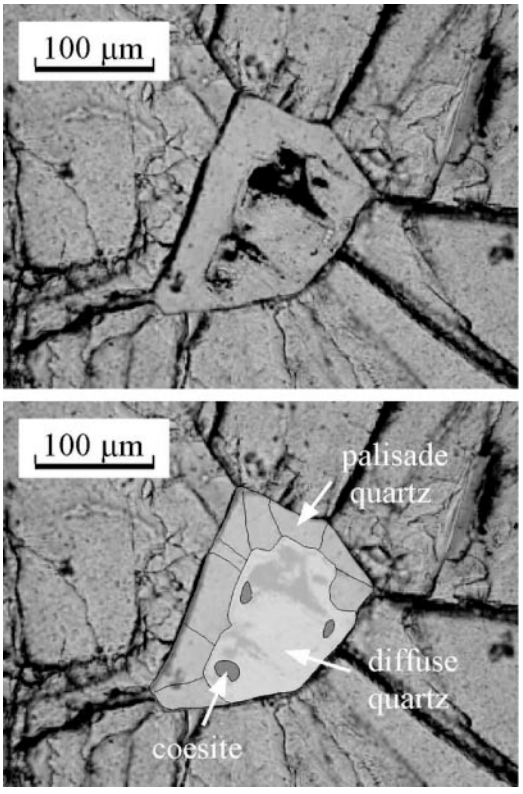

Fig. 7. Thin-section microphotograph of a coesite inclusion in a pyrope garnet host (Monts du Lyonnais UHP unit). The single crystal of coesite is surrounded by an inversion rim of polycrystalline quartz showing a radiating texture (i.e. palisade texture). Diffuse quartz develops inside the coesite grain. The radial cracks in the garnet around the inclusion should be noted. The degree of retrogression (X) can be calculated from the relative surfaces of coesite ($S_{coesite}$) and quartz (S_{quartz}), with the assumption of a spherical inclusion, using the formula $X = 1 - (S_{coesite}/S_{quartz})^{3/2}$. The degree of retrogression is estimated to be 60% when considering only the palisade quartz, and 98% when considering both palisade and diffuse quartz.

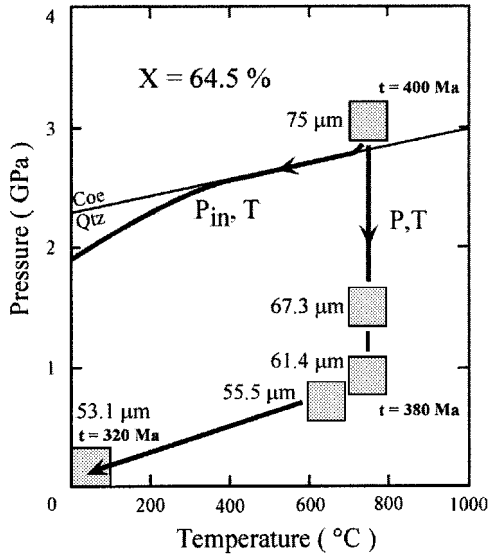

Fig. 8. Numerical modelling of the evolution of the size of a coesite inclusion in a pyrope garnet host from the Monts du Lyonnais UHP unit. P, T is the exhumation path followed by the whole UHP unit and the host pyrope (Lardeaux *et al.*, 2001); squares and t refer respectively to thermobarometric estimations and radiometric dating (in Ma) of the retrograde stages; P_{in}, T is the modelled exhumation path for the coesite inclusion. The coesite–quartz equilibrium is from Mirwald & Massonne (1980). The evolution of the size of a coesite single crystal (75 μm in radius) along the exhumation path is shown in micrometres. The final percentage of transformation (X) is in good agreement with the palisade-quartz percentage measured in the sample.

Modelling the rate of retrogression of a coesite inclusion to quartz

The numerical model has been applied to a coesite inclusion in pyrope garnet host from the Monts du Lyonnais eclogitic unit, French Massif Central (Ledru *et al.*, 1989; Mercier *et al.*, 1991). This UHP unit belongs to the western part of the Variscan chain (Matte, 1991). Coesite occurs as inclusions in garnet within eclogite lenses (Lardeaux *et al.*, 2001) and exhibits a typical retrogressive texture. The single crystal of coesite is surrounded by an inversion rim of polycrystalline quartz showing a radiating texture (i.e. palisade texture) and diffuse quartz develops inside the coesite grain (Fig. 7). In thin sections, the degree of retrogression can be estimated at 60% when considering only the palisade-textured quartz (i.e. quartz formed before the fracturing stage of garnet) and 98% when considering both palisade and diffuse quartz. The P–T–t path determined for this unit (Lardeaux *et al.*, 2001) is shown in Fig. 8. It is characterized by an initial nearly isothermal decompression at high temperature. The decompression is very fast: pressure drops from 2·8 to 0·8 GPa in less than 20 Myr, involving a high exhumation rate >1·5 mm/yr. The last part of this path is characterized by a decrease in both temperature and pressure and thereby lower exhumation rates (<0·3 mm/yr). Assuming the inclusion–host system has followed this exhumation path, the internal pressure on the inclusion and the degree of transformation from coesite to quartz are computed. The elastic parameters used in the model for pyrope and coesite, and the initial size of inclusion and host pyrope are listed in Table 4.

The calculated degree of retrogression of 64·5% (Fig. 8) agrees well with the palisade-texture percentage of 60% measured in the sample. As the P–T path modelled for the inclusion (P_{in}, T) shows a two-stage evolution, we attempted to discriminate the contribution of the elastic model and the kinetic law on the rate of retrogression. At temperatures higher that 400°C, the kinetics are fast enough such that the pressure is kept on the coesite–quartz equilibrium, whereas at

Table 4: Elastic parameters (from Gillet et al.*, 1984) and initial size of coesite and pyrope used in the model*

Coefficient	Units	Host mineral: pyrope	Coesite
K_0	Pa	$1{\cdot}5 \times 10^{11}$	$0{\cdot}96 \times 10^{11}$
$\partial K/\partial P$		5·3	8·4
$\partial K/\partial T$	Pa/K	$-2{\cdot}0 \times 10^{7}$	$-2{\cdot}0 \times 10^{7}$
α_0	K^{-1}	$21{\cdot}4 \times 10^{-6}$	$7{\cdot}3 \times 10^{-6}$
$\partial\alpha/\partial P$	$Pa^{-1}\ K^{-1}$	$-2{\cdot}0 \times 10^{7}\beta^{2*}$	$-2{\cdot}0 \times 10^{7}\beta'^{2*}$
$\partial\alpha/\partial T$	K^{-2}	$1{\cdot}1 \times 10^{-8}$	$8{\cdot}5 \times 10^{-9}$
μ_0	Pa	$9{\cdot}0 \times 10^{10}$	—
$\partial\mu/\partial P$		1·5	—
$\partial\mu/\partial T$	Pa/K	$-1{\cdot}0 \times 10^{7}$	—
Inclusion radius $R_{i0} = 75 \times 10^{-6}$ m			
Garnet radius $R = 2{\cdot}5 \times 10^{-3}$ m			

*β and β′ are the inverse of incompressibility $K(T,P)$.

temperatures below 400°C, the P_{in},T curve moves away from the coesite–quartz equilibrium, to lower pressures. This indicates that the transformation is not efficient in maintaining sufficiently high pressures on the inclusion. Consequently, above 400°C the retrogression is mainly controlled by the elastic model, whereas the kinetics of the coesite–quartz transition is the controlling factor at lower temperature. Using the kinetic parameters of Mosenfelder & Bohlen (1997) in our model would shift this temperature limit of 400°C only 50–100°C higher. For P–T paths showing decompression at high temperature (as in the Monts du Lyonnais UHP unit) the assumption of instantaneous transformation (Gillet *et al.*, 1984; Van der Molen & Van Roermund, 1986) is valid. On the other hand, for P–T paths characterized by decompression at low temperature (near or below 400°C) this assumption could lead to an overestimation of the degree of retrogression.

Consequently, the recognition of coesite in metamorphic rocks cannot be systematically considered as evidence for a 'cold' retromorphic path (i.e. with significant cooling during decompression); as demonstrated by the occurrence of relict coesite in the Monts du Lyonnais. This is consistent with the discovery of coesite in granulite retrogressed from eclogite in Weihai, eastern China (Wang *et al.*, 1993).

Factors acting upon the preservation of coesite

This model provides the opportunity to investigate the influence of several factors that could contribute to the survival of coesite during exhumation. In this section, the effects of the type of host mineral, the P–T conditions at which the inclusion–host system formed, and the rupture of the host mineral are discussed qualitatively.

In nature, coesite inclusions occur in various host minerals: garnet, pyroxene, kyanite, titanite, zircon, rutile and diamond (e.g. Liou *et al.*, 1998), which differ in their structures and elastic properties. In particular, the bulk modulus (K_0) ranges from 129 GPa for omphacite to 150 GPa for pyrope, 227 GPa for zircon and 444 GPa for diamond (e.g. Knittle, 1995). Increasing the bulk modulus of the host phase increases the 'pressure vessel' effect, and following our model, the coesite inclusion will consequently reach the coesite–quartz equilibrium at lower temperatures. The amount of quartz retrogressed will thus be reduced. This is in agreement with the measurements by Parkinson & Katayama (1999) of present-day ultrahigh-pressure conditions (19–23 kbar) in coesite inclusions in zircon. The P–T conditions at which the inclusion–host system was formed influence also the preservation of coesite. Because, for a given temperature, the estimated pressure of trapping of the inclusion is a minimum value, higher pressures cannot be excluded. A higher pressure of formation for the inclusion–host system would delay the transformation of coesite to quartz to lower temperatures. Consequently, the higher the pressure of trapping of the inclusion, the more coesite will be preserved. Nevertheless, the survival of coesite is also strongly dependent on the rupture of the host mineral. Our model does not take into account this effect, which would cause a strong decompression of the coesite inclusion, leading to the nucleation and growth of diffuse quartz. As a result of the exponential decrease in retrogression kinetics with temperature, the lower the temperature of fracture, the more coesite will be preserved. The conditions at which fracture takes place are difficult to evaluate as they depend on numerous factors, including the P–T conditions and the exact chemical composition of the host mineral. Van der Molen & Van Roermund (1986) estimated that the internal pressure has to exceed three times the external pressure before fracture can occur. Nishiyama (1998) used this failure criterion to calculate the temperature at which rupture would happen for various exhumation P–T paths. Modelling of the internal pressure (Fig. 8) suggests that slow kinetics would reduce the pressure differential between the inclusion and the host, and thus delay fracture to lower temperatures, where the transformation is sluggish.

Hence, the survival of coesite results from a process combining the 'pressure vessel' effect of the host mineral, the kinetics of the reaction and the conditions

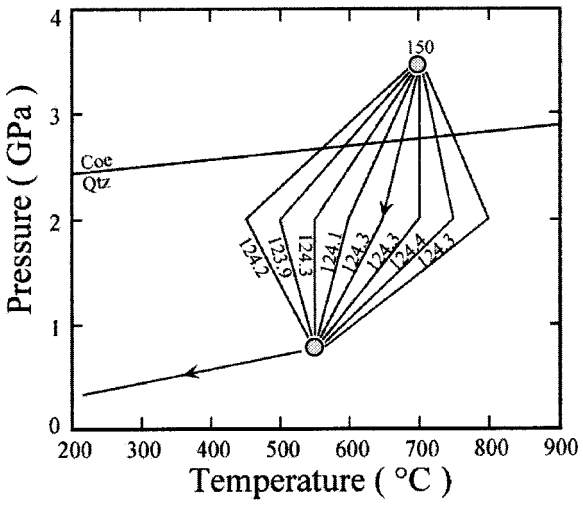

Fig. 9. Modelled coesite inclusion sizes along several different exhumation paths passing through two P–T points (circles). The radius of the coesite grains at the HP and LP points is indicated in micrometres. The decompression rate is constant at 0·3 GPa/Myr. The quartz–coesite equilibrium is from Mirwald & Massonne (1980). The inclusion radius at 0·8 GPa, 550°C is close to 124 μm whatever the path followed, showing the lack of influence of P–T path shape on retrogression at temperatures higher that 400°C.

of subsequent fracturing. Our model provides information about the coupling between the two first parameters. The conditions under which the host mineral fractures need further investigation for a better understanding of the coesite preservation.

Influence of *P–T* path shape and exhumation rate upon retrograde reaction

In a further development of the above model, we investigated the influence of P–T path shape and exhumation rate upon transformation of coesite to quartz. P–T–t paths are usually obtained by linear interpolation between thermobarometric and geochronological data points. This interpolation is arbitrary and cooler or hotter, slower or faster paths passing through the data points are also possible. The degree of retrogression of natural coesite samples might help to improve this interpolation.

To test this hypothesis, we have computed the size of a 150 μm coesite inclusion in pyrope along several exhumation paths (Fig. 9) passing through lower or higher temperatures than the path resulting from linear interpolation. The calculated retrogression rates do not show significant variations. In all cases the inclusion radius at 0·8 GPa, 550°C is close to 124 μm. This can be explained by the fact that, at such temperatures, retrogression is mainly controlled by the elastic role played by the host mineral (see previous section). Consequently, as elastic deformation is a reversible process, the amount of quartz produced is independent of the P–T path followed and depends only on the initial and final P–T conditions. For the same reason, varying exhumation rates along these paths would have no influence on the degree of retrogression.

The coesite–quartz transition appears to be too fast to use the percentage of retrogression of coesite inclusions to constrain P–T–t paths more precisely. However, the model developed in this study could be used with success for polymorphic phase transitions characterized by slower kinetics, i.e. with a higher temperature below which kinetics is the controlling factor. Reaction kinetics might thus be a useful tool for studying exhumation, as it provides a continuous record from the HP–LP phase equilibrium to the surface. As the conversion from the HP to the LP polymorph depends on both P–T path shapes and exhumation rates, reaction rate data must be used in parallel with thermobarometric and geochronological data. Consequently, one of these two sets of variables must be known (or fixed) to provide information on the other. Moreover, the solution obtained would not be unique, as a range of exhumation rates or P–T paths can account for a given degree of retrogression. Hence, reaction kinetics will define a 'trend' or family of P–T–t paths, which will be of great interest when compared with the exhumation models.

CONCLUSION

The analysis of transformation–time data based on simple models of nucleation and growth at grain boundaries proves that the kinetics of the coesite–quartz transition is controlled by thermally activated growth processes. The coesite → quartz kinetic law, deduced from these laboratory experiments, can be used to study the preservation of coesite in UHP rocks, as the texture of coesite inclusions in host minerals such as garnet suggests high nucleation rates at geological time scales. Coupling this kinetic law with an 'inclusion in a host' elastic model allows us to calculate the degree of retrogression of a coesite inclusion during its ascent to the Earth's surface. Application to the Monts du Lyonnais UHP units shows that retrogression is mainly controlled by the elastic behaviour of the host mineral above 400°C; whereas reaction kinetics is the controlling factor below this temperature.

Ultimately, such a model can be used to constrain exhumation P–T–t paths from the percentage of retrogression of inclusions even if the coesite–quartz transition appears too fast for this purpose, although this approach might be successful for more sluggish transitions. Reaction kinetics would thus be an additional

approach for studying exhumation mechanisms of UHP metamorphic rocks.

ACKNOWLEDGEMENTS

This study benefited from the support of J. P. Itié and Y. Le Godec (Lab. Physique Milieux Condensés, Paris VI) during X-ray diffraction experiments at LURE. J. Matas helped in thermodynamic calculations. Careful and constructive reviews by C. Chopin, H. P. Liermann and P. J. O'Brien are also gratefully acknowledged.

REFERENCES

Ahnert, F. (1970). Functional relationships between denudation, relief, and uplift in large mid-latitude drainage basins. *American Journal of Science* **268**, 243–263.

Andersen, T. B. & Jamveit, B. (1990) Uplift of deep crust during orogenic extensional collapse: a model based on field studies in the Sogn–Sunnfjord region of Western Norway. *Tectonics* **9**, 1097–1111.

Avrami, M. (1939). Kinetics of phase change. *Journal of Chemistry and Physics* **7**, 1103–1112.

Babich, Y. V., Doroshev, A. M. & Malinovsky, I. Y. (1989). Thermally activated transformation of coesite. *Geologiya i Geofizika* **1989**(2), 140–144.

Besson, J. M., Nelmes, R. J. & Hamel, G. (1992). Neutron powder diffraction above 10 GPa. *Physica B, Condensed Matter* **180 & 181B**, 907–923.

Bose, K. & Ganguly, J. (1995). Quartz–coesite transition revisited: reversed experimental determination at 500–1200°C and retrieved thermochemical properties. *American Mineralogist* **80**, 231–238.

Cahn, J. W. (1956). The kinetics of grain boundary nucleated reactions. *Acta Metallica* **4**, 449–459.

Carswell, D. A. (eds) (2000). *Ultra-High Pressure Metamorphic Rocks*. *Lithos*, Special Issue, **52**.

Chemenda, A. I., Mattauer, M., Malavieille, J. & Bokum, A. N. (1995). A mechanism for syncollisional rock exhumation and associated normal faulting: results from physical modelling. *Earth and Planetary Science Letters* **132**, 225–232.

Chopin, C. (1984). Coesite and pure pyrope in high-grade blueschists of Western Alps: a first record and some consequences. *Contributions to Mineralogy and Petrology* **86**, 107–118.

Cloos, M. (1982). Flow melanges: numerical modeling and geologic constraints on their origin in the Franciscan subduction complex, California. *Geological Society of America Bulletin* **93**, 330–345.

Coleman, R. G. & Wang, X. (eds) (1995). *Ultrahigh Pressure Metamorphism*. Cambridge: Cambrige University Press.

Cowan, D. S. & Silling, R. M. (1978). A dynamic model of accretion at trenches and its implications for the tectonic evolution of subduction complexes. *Journal of Geophysical Research* **83**, 5389–5396.

Dobrzhinestskaya, L. E., Eide, E. A., Larsen, R. B., Sturt, B. A., Tronnes, R. G., Smith, D. C., Taylor, W. R. & Posukhova, T. V. (1995). Microdiamond in high-grade metamorphic rocks of the Western Gneiss region, Norway. *Geology* **23**, 597–600.

Duchêne, S., Lardeaux, J. M. & Albarède, F. (1997). Exhumation of eclogites: insights from depth–time path analysis. *Tectonophysics* **280**, 125–140.

England, P. & Molnar, P. (1990). Surface uplift, uplift of rocks, and exhumation of rocks. *Geology* **18**, 1173–1177.

Gillet, P., Ingrin, J. & Chopin, C. (1984). Coesite in subducted continental crust: *P–T* history deduced from an elastic model. *Earth and Planetary Science Letters* **70**, 426–436.

Guillot, S., Hattori, K. & de Sigoyer, J. (2000). Mantle wedge serpentinization and exhumation of eclogites: insights from eastern Ladakh, northwest Himalaya. *Geology* **28**, 199–202.

Hammi, Y. (1995). Calcul par éléments finis de l'équilibre thermique d'un four à résistance de graphite. DEA report, Paris VII University.

Knittle, E. (1995). Static compression measurements of equations of state. In: *Mineral Physics and Crystallography—Handbook of Physical Constants*. Washington, DC: American Geophysical Union, pp. 98–142.

Lardeaux, J. M., Ledru, P., Daniel, I. & Duchêne, S. (2001). The Variscan French Massif Central—a new addition to the ultra-high pressure metamorphic 'club': exhumation processes and geodynamic consequences. *Tectonophysics* **332**, 143–167.

Lasaga, A. C. (1998). *Kinetic Theory in the Earth Sciences*. Princeton, NJ: Princeton University Press.

Ledru, P., Lardeaux, J. M., Santallier, D., Autran, A., Quenardel, J. M., Flo'ch, J. P., Lerouge, G., Maillet, N., Marchand, J. & Ploquin, A. (1989). Où sont les nappes dans le Massif Central français? *Bulletin de la Société Géologique de France* **8**, 605–618.

Le Godec, Y. (1999). Étude du nitrure de bore sous hautes pression et température. Ph.D thesis, Paris VII University.

Liou, J. G., Zhang, R. Y., Ernst, W. G., Rumble, D. & Maruyama, S. (1998). High-pressure minerals from deeply subducted metamorphic rocks. In: Hemley, R. J. (ed.) *Ultrahigh Pressure Mineralogy. Mineralogical Society of America, Reviews in Mineralogy* **37**, 33–96.

Liu, M. & Yund, R. A. (1993). Transformation kinetics of polycrystalline aragonite to calcite: new experimental data, modeling and implications. *Contributions to Mineralogy and Petrology* **114**, 465–478.

Matte, P. (1991). Accretionary history of the Variscan belt in western Europe. *Tectonophysics* **196**, 309–337.

Mercier, L., Lardeaux, J. M. & Davy, P. (1991). On the tectonic significance of retrograde *P–T–t* paths in eclogites of the French Massif Central. *Tectonics* **10**, 131–140.

Mirwald, P. M. & Massonne, H. J. (1980). The low–high quartz–coesite transition to 40 kbar between 600°C and 1600°C and some reconnaissance on the effect of $NaAlO_2$ component on the low quartz–coesite transition. *Journal of Geophysical Research* **85**, 6983–6990.

Mosenfelder, J. L. & Bohlen, S. R. (1997). Kinetics of the coesite to quartz transformation. *Earth and Planetary Science Letters* **153**, 133–147.

Nishiyama, T. (1998). Kinetic modeling of the coesite–quartz transition in an elastic field and its implication for the exhumation of ultrahigh-pressure metamorphic rocks. *Island Arc* **7**, 70–81.

Parkinson, C. D. & Katayama, I. (1999). Present-day ultrahigh-pressure conditions of coesite inclusions in zircon and garnet: evidence from laser Raman microspectroscopy. *Geology* **27**, 979–982.

Platt, J. P. (1986). Dynamics of orogenic wedges and the uplift of high-pressure metamorphic rocks. *Geological Society of America Bulletin* **97**, 1037–1053.

Platt, J. P. (1993). Exhumation of high pressure rocks: a review of concepts and processes. *Terra Nova* **5**, 119–133.

Robie, R. A., Hemingway, B. S. & Fisher, J. R. (1978). Thermodynamic properties of minerals and related substances at 298·15 K and 1 bar pressure and at higher temperatures. *US Geological Survey Bulletin* **1452**, 456 pp.

Rubie, D. C., Tsuchida, Y., Yagi, T., Utsumi, W., Kikegawa, T., Shimomura, O. & Brearley, A. J. (1990). An *in situ* X ray diffraction study of the kinetics of the Ni_2SiO_4 olivine–spinel transformation. *Journal of Geophysical Research* **95**, 15829–15844.

Saxena, S. K., Chatterjee, N., Fei, Y. & Shen, G. (1993). *Thermodynamic Data on Oxides and Silicates*. New York: Springer.

Skelton, E. F., Quadri, S. B., Webb, A. W., Lee, C. W. & Kirkland, J. P. (1983). Improved system for energy dispersive X-ray diffraction with synchrotron radiation. *Review of Scientific Instruments* **54**, 403–409.

Smith, D. C. (1984). Coesite in clinopyroxene in the Caledonides and its implications for geodynamics. *Nature* **310**, 641–644.

Sobolev, N. V. & Shatsky, V. S. (1990). Diamond inclusions in garnets from metamorphic rocks: a new environment for diamond formation. *Nature* **343**, 742–746.

Turnbull, D. (1956). Phase changes. *Solid State Physics* **3**, 225–306.

Van der Molen, I. & Van Roermund, H. L. M. (1986). The pressure path of solid inclusions in minerals: the retention of coesite inclusions during uplift. *Lithos* **19**, 317–324.

Vinet, P., Ferrante, J., Smith, J. R. & Rose, J. H. (1987). Compressibility of solids. *Journal of Geophysical Research* **92**, 9319–9325.

Wang, Q., Ishiwatari, A., Zhongyan, Z., Hirajima, T., Hiramitsu, N., Enami, M., Zhai, M., Li, J. & Cong, B. (1993). Coesite-bearing granulite retrograded from eclogite in Weihai, eastern China. *European Journal of Mineralogy* **5**, 141–152.

Will, G. & Lauterjung, J. (1987). The kinetics of the pressure induced olivine–spinel phase transition of Mg_2GeO_4. In: Manghnani, M. H. & Syono, Y. (eds) *High-Pressure Research in Mineral Physics*. *Geophysical Monograph, American Geophysical Union* **39**, 177–186.

Zhang, Y. (1998). Mechanical and phase equilibria in inclusion–host systems. *Earth and Planetary Science Letters* **157**, 209–222.

Zinn, P., Lauterjung, J. & Hinze, E. (1995). Kinetic studies of the crystallisation of coesite using synchrotron radiation. *Nuclear Instruments and Methods in Physics Research B* **97**, 89–91.

Zinn, P., Hinze, E., Lauterjung, J. & Wirth, R. (1997*a*). Kinetic and microstructural studies of the quartz–coesite phase transition. *Physics and Chemistry of the Earth* **22**, 105–111.

Zinn, P., Lauterjung, J., Wirth, R. & Hinze, E. (1997*b*). Kinetic and microstructural studies of the crystallisation of coesite from quartz at high pressure. *Zeitschrift für Kristallographie* **212**, 691–698.